

PHYSICAL INVESTIGATIONS OF NANOPHOTONIC LiNbO_3 FILMS FOR PHOTONIC APPLICATIONS

S. M. TALEB, M. A. FAKHRI*, S. A. ADNAN

Laser and Optoelectronic Department, University of Technology, 10066 Baghdad, Iraq

The nanocrystalline structure of Lithium niobate (LiNbO_3) was prepared and deposited onto substrate made of quartz by utilize pulse laser deposition technique. The effect of substrate temperature on the structural, optical and morphological properties of lithium niobate photonic film grown was studied. The chemical mixture was prepared by mixing the raw material (Li_2CO_3 , Nb_2O_5) with Ethanol liquid without any further purification, at time of stirrer 3hrs but without heating, then annealing process the formed material at 1000°C for 4hrs. We characterized and analyzed the LiNbO_3 nanostructure thin films by utilize Ultra-Violet Visible (UV-vis), X-Ray Diffraction (XRD) and Atomic Force Microscopy (AFM). The UV-vis measurements show that, when the substrate temperature increases, the values of transmission, absorption and energy band gap will decreased, but the values of reflection and refractive index will increased. While, the XRD measurements show that, the LiNbO_3 structure will be more purity and crystalline with rising the substrate temperature, because the intensity of phase 2θ at value of 34.8° , 40.06° and 48.48° correspond to (110), (113) and (024) planes will be disappeared when the substrate temperature increases. Also, the AFM measurements show that, when the substrate temperature increased, the structure of film started to crystallization to be more homogeneous, smooth and uniform, while the surface roughness and grain size increased also with increase the substrate temperature. That means the LiNbO_3 thin film prepared at substrate temperatures 300°C give the best result for manufacture the optical waveguide.

(Received April 11, 2019; Accepted August 26, 2019)

Keywords: LiNbO_3 , Thin Films, Optical properties, Structural properties, Morphological properties

1. Introduction

Lithium Niobate (LiNbO_3) represent a very important optical material, because of its excellent electro and acousto-optical properties [1], it is widely utilized by the industry of photonics. Also, LiNbO_3 is a suitable choice for optical wave guide applications [2], due to it offers a large and prominent optical quality. Furthermore, LiNbO_3 is also represent the ferroelectric material very important, due to its photo-refractive properties, piezoelectric, pyroelectric and electro optical [3]. For photonic and optoelectronic applications LiNbO_3 widely utilized as an essential and effective material [4-5]. LiNbO_3 is a very promising material to fabricate the integrated optical devices [6-7] due to its superior optical properties which suitable for various optical applications. LiNbO_3 has more advantages than the bulk LiNbO_3 , such as fabrication of the multilayer structures, the potential of producing step index, miniaturization and integration of these devices [8]. In addition to that, in nonlinear optics, LiNbO_3 is widely used for telecommunication, for electro-optic modulation and for frequency conversion [9].

We have been studied LiNbO_3 nanostructure to use it in the integrated form with the piezoelectric, pyroelectric [10], also the nonlinear optical properties, that make it the perfect material to manufacture the surface acoustic wave (SAW) [11], optoelectronic devices [12-13]. Due to mechanical robustness, optical homogeneity [14], integrated optics with lasers, good availability, modulators [15], and filters on a single LN wafer [16], that make LiNbO_3 the

*Corresponding author: 140017@uotechnology.edu.iq

promising material for optical devices. Also, LiNbO_3 material is a suitable material in optical communication systems, which are widely used for applications in microwave telecommunications, optical switches, beam deflectors, memory units, electro optics, modulators, waveguides, second harmonic generation and surface acoustic waves (SAW) devices [17-18], because it has high electro-optical coefficient and low optical losses. LiNbO_3 is also represent the attractive host material for application in photonic crystal devices [19], due to its remarkable linear and nonlinear optical properties, chemical and mechanical stability.

The structure of LiNbO_3 is hexagonal structure with lattice parameters $a = 0.5147$ nm and $c = 1.3862$ nm [20]. LiNbO_3 single crystal has large second-order nonlinearities [21]. That make it one of the key materials for optical based technologies. In addition, LiNbO_3 has several potential advantages from commercial or technological view point of integrated optics [22]. LiNbO_3 is a very charming material in fabrication of optical wave-guide devices [23-24], surface acoustic wave [25] and optoelectronic devices [26]. Optical waveguide is essential for the photonic device, and it is used to change the size of light spot in order to have a superior coupling efficiency (less loss) between the two sections with different refractive index and different cross sections [27].

In past years, LiNbO_3 waveguides are widely utilized in many functional acousto optic and electro-optic devices [28], where the structure of waveguides are very important for many integrated-optic devices. There are stringent requirements imposed on waveguide films Imperfections for waveguide application which represent porosity, refractive-index inhomogeneity [29-30], and roughness of surface, which plays a very important role in the performance of the device [31-32]. There are various techniques to prepared LiNbO_3 thin film such as liquid phase epitaxial (LPE) [33], metal organic chemical vapor deposition (MOCVD) [34], soft- chemistry [35], pulse methods [36], sol-gel [37-38], hydrothermal methods [39-40], Ion Beam Sputtering [41], RF magnetron sputtering [42], and pulsed laser deposition (PLD) [43].

Pulse laser deposition technique is widely used in the deposition of several materials such as oxides, nitrides, superconductors, etc. [44]. PLD represent a very important technique to prepared thin films, because of its advantages such a possibility to use different substrate materials [45-46], high reproducibility, control of the films growth rate, low cost, low impurity concentration in the composition of deposited films and simplicity, the possibility of prepared the high quality thin films at low growth temperatures. This technology also allows transfer a stoichiometric material from the target towards the substrates surfaces in case of multicomponent targets. These advantages and others make this technique one of the most powerful techniques for thin film research.

The quality of thin film deposited depends on many parameters such as laser energy, substrate type and temperature, laser wavelength, angle of deposition, number of laser pulses, gas pressure, fluency, target-substrate distance, and thermo physical properties of the target material which include density, mass, absorption coefficient, etc. So that, when these parameters are optimized this helps to get high quality thin film for the optical waveguide application. This work report the preparation of LiNbO_3 nanostructures at wavelength 532 nm by using the pulse laser deposition technique on substrates made of quartz. Due to the Quartz substrate agree with a many of optical properties, processing techniques, that make it suitable choice for many deposition processes.

The effect of the substrate temperature on the structural, optical and morphological properties of the thin film prepared was analyzed by using UV visible, X-ray diffraction and atomic force microscopy AFM; which represent the important section of this work to find the possibility applicability LiNbO_3 thin film in optical waveguides. Where the optical characteristics, crystallization, purity, homogeneity, surface roughness, grain size for LiNbO_3 thin film, these parameters and other will affect the efficiency of the optical waveguides. The UV visible is measured to find the best value of refractive index because of refraction coefficients between the base and deposited films will assure access to total internal reflection to give the best result of optical waveguide, the XRD is measured to characterize the structural properties and find the highest value of the intensity, and the AFM is measured to analyze the surface topography and grain size.

2. Experiment

LiNbO₃ nanostructured thin film was prepared by using pulsed laser deposition technique on the quartz substrates. The quartz substrates were cleaned before performed the deposition process. Where these steps of cleaning represent a very important to elimination the impurities and fingerprints of the quartz substrates. The quartz is immersing into solution of water and soap for 10 mins with cleaning by the hand. After that rinse it with water several times, then placing it in Ethanol liquid for 5 mins. Finally, drying it under the hot air. The solution is prepared by mixing raw materials ultra-purity which are: Lithium carbonate (Li₂CO₃), Niobium oxide (Nb₂O₅) and Ethanol liquid (C₂H₅OH) without any further purification. In order to maximize the formation of the stoichiometry of LiNbO₃ phase we kept the molar ratio between the main raw materials (Li₂CO₃, Nb₂O₅) 1:1 with the following weights (Li₂CO₃= 5gm, Nb₂O₅= 5gm, C₂H₅OH=30ml). The first step is dissolving the raw materials (Li₂CO₃, Nb₂O₅) in C₂H₅OH without heating but with stirring for 3hrs by the magnetic stirrer device. After finishing the mixing process, the mixture was kept in room temperature for 48hrs for drying purposes. After 48hrs, the mixture was observed separate where the material was deposited at the bottom and the liquid at the top. The material formed was annealed for 4hrs at a temperature of 1000C°. After the annealed process the material was milled by the manual method to convert it into a powder. Finally, the powder material is compressed by applying a pressure of 15 tons to produce a disk with 2cm diameter and 1cm height. See Fig 1 (a-b).



Fig. 1. a- the powder of lithium niobate LiNbO₃. b- The target before the annealing process.

All these steps are shown in Fig 2, which represent the flow chart of deposition steps. By using Ultr-Violet visible (UV-vis) spectrophotometer (Shimadzu UV-Vis 1800, Japan) in wavelength range (200–1200) nm we calculated via transmittance (T) spectrum the optical properties of thin film which represent the optical absorbance (A), Optical band gap (E_g), Reflectance (R), Refractive index (n). Then by the X-ray diffraction (XRD), (X'Pert Pro MRD PW3040 system diffractometer, PANalytical Company, Netherlands) system equipped with Cu-K α-radiation of wavelength $\lambda = 0.15418$ nm, at 40 kV and 30 mA we studied structure properties of this films at same wavelength range. Also, by atomic force microscopy (AFM) (SPM-9600, Scanning Probe Microscope, Shimadzu, Japan) we measured the roughness, regularity and grain size of LiNbO₃ surface.

3. Results and discussion

LiNbO₃ nanostructure thin films which prepared by using PLD technique on quartz substrates at the two different temperatures (250C°-300C°) and wavelength 532 nm were characterized and analyzed by UV-Vis spectrophotometer, X-ray Diffraction (XRD) and atomic force microscopy (AFM). The optical properties of LiNbO₃ thin films were determined from the transmission measurements in the wavelength range (200-1200) nm. Figure 3 shows the optical transmission of LiNbO₃ nanostructure at substrate temperature (250C°-300C°).

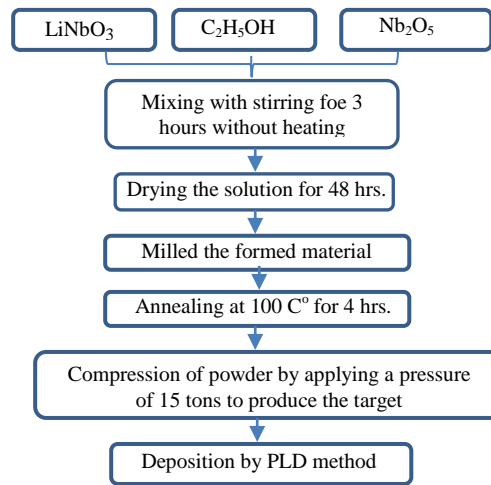


Fig. 2. Flow chart of LiNbO_3 nanophotonic thin film preparation process.

From this figure we can note that the optical transmission decreases when the substrate temperature increases. Where the transmission values are (88-78) % corresponding to substrate temperature (250°C - 300°C). The high value of transmittance is attributed to the excessive (LiNbO_3) ions at interstitial sites that increased its transparency level. The same case applies to optical absorption, where the values of absorption also increase when the substrate temperature decreases as shown in Figure 4. These values are about (2.7-3.3) at substrate temperatures (300°C - 250°C) with the same wavelength (532 nm). As a function of photon energy we established the optical band gap E_g which was found by plotting the curve between $(ah\nu)^2$ and $(h\nu)$ as shown in Figure 5. The E_g which was calculated is about (4.4-4.7) eV corresponding to the (300°C - 250°C) substrate temperature respectively, at wavelength 532 nm. That means when the substrate temperature increases, the band gap energy decreases and vice versa. From the absorption and the transmission spectra according to the relation; $R+T+A=1$, we calculated the optical reflectance (R) of LiNbO_3 nanostructures as shown in Figure 6. This figure shows the reflectance of LiNbO_3 in the wavelength range (200-1200) nm at two different substrate temperatures. We can note that the values of the R% increase when the substrate temperature increases, these values are about (11-20) % corresponding to substrate temperature (250°C - 300°C). From the transmittance spectrum as a function of the wavelength in the range (200-1200) nm, we determined the refractive index (n) at the two different substrate temperatures. There is a decrease in the refractive index when the substrate temperature decreases, which is (2.49-2.63) at substrate temperature (250°C - 300°C) as shown in Figure 7. When the value of refractive index is high, this makes it more suitable for manufacturing the optical waveguides [48-52].

The effect of substrate temperature on the XRD results of LiNbO_3 nanostructures deposited on quartz substrate is shown in Figure 8. With lattice parameters $a = 5.145$, $c = 13.858$, we found that the LiNbO_3 has a hexagonal structure. It is observed from this figure that the LiNbO_3 crystal structure has diffraction peaks at $2\theta = 23.66^\circ$, 32.66° , 34.8° , 38.94° , 40.06° , 42.52° , 48.48° , 53.22° and 62.38° corresponding to (012), (104), (110), (006), (113), (202), (024), (116), and (300) planes. X-ray diffraction distinctly indicates that there is a tiny quantity of the subaltern LiNbO_3 incomplete stage (LiNb_3O_8 , δ phase) when the substrate temperature increased to 300°C , at 2θ values of 34.8° , 40.06° and 48.48° corresponding to (110), (113) and (024) planes. Where, the intensity of these phases disappeared when the substrate temperature increased. Where the reaction between oxygen and LiNbO_3 led to the origin of this phase. The intensity of the peak arrived to a value of 1640 at substrate temperature 300°C compared to the intensity of the peak at substrate temperature 250°C which arrived to a value of 720 in the performed phase with (012) orientation, that means the LiNbO_3 structure will be more pure and crystalline when the substrate temperature

increasing. Also, When the temperature of the substrate increases, this leads to an increase the average of particle size because of the crystals will be rearrangement and restructuring to improvement the properties of the structural and to get High rate of purity of LiNbO_3 nano film. So if we want to manufacture the optical waveguide with high efficiency, we must be to get LiNbO_3 material with high- purity. The phase of substrate temperature 300C° is higher than that of substrate temperature 250C° . From these results we can noted that the behavior of nanophotonic at substrate temperature 300C° is much better than the substrate temperature 250C° , where it found it more clearer and more crystallization. Accordingly, The optical waveguide manufacturing will be better when using thin film prepared at the substrate temperature 300C° .

The images of AFM for LiNbO_3 nanostructure thin film which prepared at the different substrate temperature (250C° - 300C°) shown on Figure 9 (a-b) with the thick and regular surface, which appear the increasing in surface roughness and grain size when the substrate temperature increase. within the scanning area ($2\ \mu\text{m} \times 2\ \mu\text{m}$) by the AFM micrographs we noted that the topography of the surface for LiNbO_3 nanostructures prove that the distributed of the grains are uniformly and the columnar grains extending upwards. Where the characteristic of the surface is very important, Where it can be observe that the thin film prepared at substrate temperature 300C° is more regular, homogeneous and soft compared to thin film prepared at substrate temperature 250C° . The AFM result show that the roughness of the surface, roughness average and average diameter of grain size increasing when the substrate temperature increase, where analysis shows that surface roughness values are (0.624-3.23) nm, roughness avg (0.54-2.77) nm and the avg. diameter of grain size (70.39 to 108.5) nm for LiNbO_3 thin film deposited at substrate temperature (250C° - 300C°) respectively, so the surface roughness increases with substrate temperature due to the difficulty of Solubility, while a large grain appear correlation to increased the substrate temperature, this is due to increase particulate ablation during PLD process, Figure 10 (a-b) show the grain size. That means the substrate temperature effect on the size of grains and roughness of the surface. Also, increasing the substrate temperature affect positively on the size of grain that guide to tarnished the surface to become more smooth, uniform and dense.

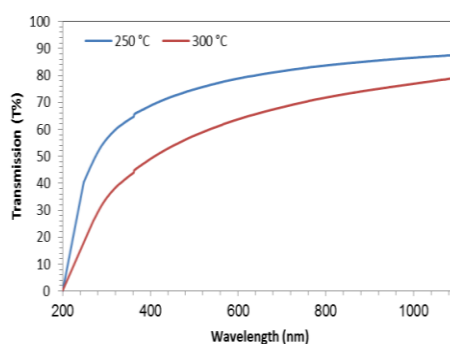


Fig. 3. The optical transmission of LiNbO_3 at different substrate temperature.

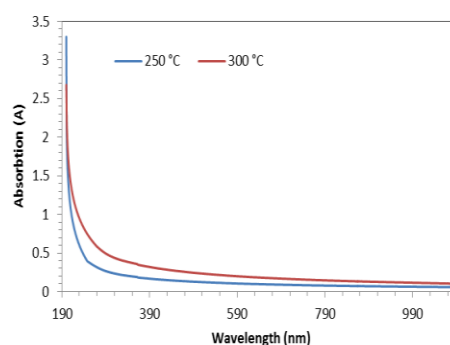


Fig. 4. The optical absorption of LiNbO_3 at different substrate temperature.

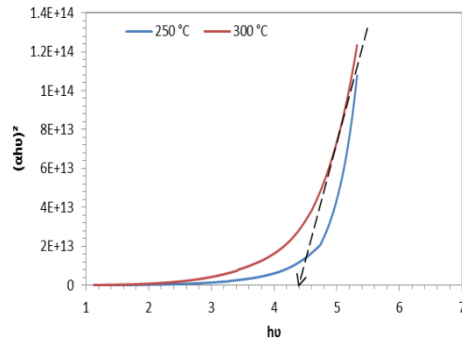


Fig. 5. The optical band gap (E_g) of LiNbO_3 at different substrate temperature.

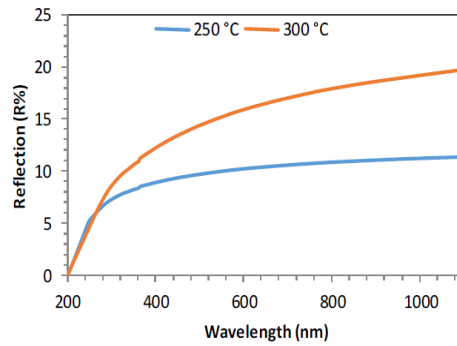


Fig. 6. The optical Reflection of LiNbO_3 at different substrate temperature.

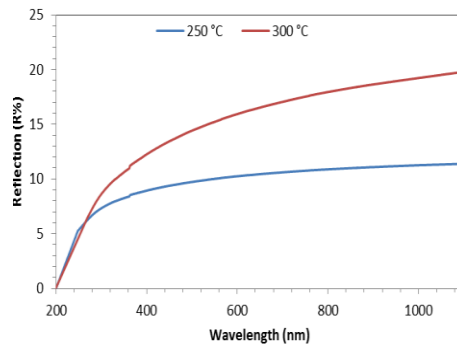


Fig. 7. Refractive index of LiNbO_3 at different substrate temperature.

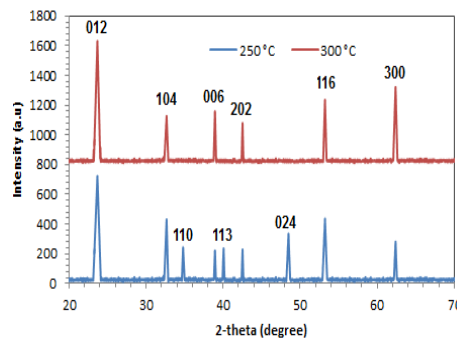


Fig. 8. XRD patterns of LiNbO_3 at different substrate temperature.

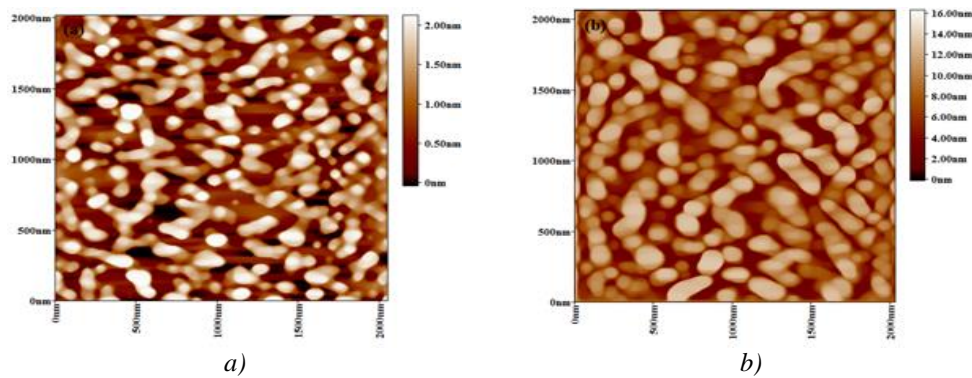


Fig. 9. The images of AFM for LiNbO_3 at different substrate temperature. (a) 250°C (b) 300°C .

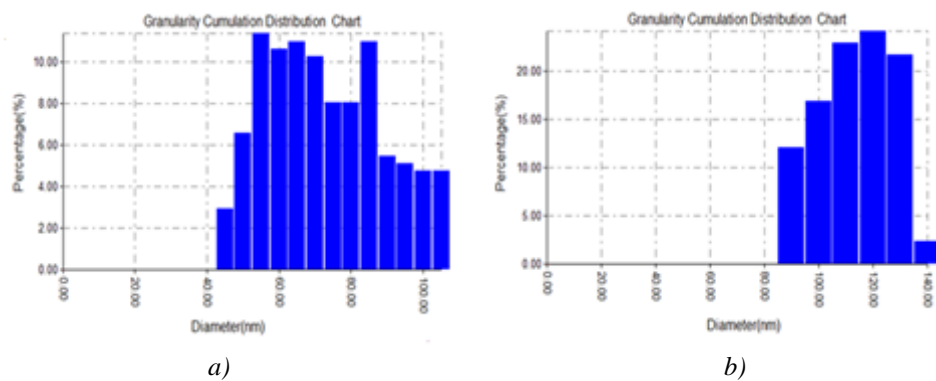


Fig. 10. AFM grain size of LiNbO_3 nanostructures at two different substrate temperature. (a) 250°C (b) 300°C .

4. Conclusions

Nanostructure thin films of LiNbO_3 were prepared by PLD technique using a Q-switched 532 nm Nd:YAG laser on the quartz substrates with two different substrate temperature (250°C - 300°C). From the results presented in this report, we note that:- The optical properties give highest values of transmission, absorption and band gap energy when the substrate temperature decreased to 250°C . By changed the growth parameters, the optical properties of the thin films could be optimized, which represent the important advance in thin film manufacturing. From the transmission and the absorption spectrums, we calculated the optical reflectance. While from only the transmission spectrum, we determined the refractive index. Where, both them achieve the highest values at substrate temperature 300°C . The higher of the refractive index value, the more suitable it is to manufacture the optical waveguides. From the results of XRD, we found the LiNbO_3 have a polycrystalline structure in nature, due to it have various peaks in various plane orientations. The peak at $2\theta = 23.66$ with (012) orientation have the intensity increasing dramatically with increased the substrate temperature to 300°C , which arrived to the value 1640.

The structure is become more crystalline and more purity when the substrate temperature increased. So, the improvement in the crystal structure of LiNbO_3 is obtained by increasing the substrate temperature to 300°C through the deposition process. AFM results showed that the surface roughness, the average roughness and the grain size increases with increasing the substrate temperature, where the grain size of prepared nanoparticles observed at the surface depends on the substrate temperature. Also the topographic images found more regular, homogeneous and downy with strengthen the nanophotonic structure. That means the AFM ensures the improvement in the film morphology with increasing the substrate temperature. Finally from all these results, we can

conclusion the optimum condition to manufacturing the optical waveguide is the substrate temperature 300C°.

References

- [1] E. Marenga, C. Aruta, E. Fanelli, M. Barra, P. Pernice, A. Aronne, *Journal of Solid State Chemistry* **182**, 1229 (2009).
- [2] E. T. Salim, M. A. Fakhri, Ismail, R.A., Abdulwahhab, A.W., Salim, Z.T., Munshid, M.A., Hashim, U., *Superlattices and Microstructures* **128**, 67 (2019).
- [3] Fakhri, M.A., Salim, E.T., Wahid, M.H.A., Abdulwahhab, A.W., Hashim, U., Salim, Z.T., *Optik* **180**, 768 (2019).
- [4] Agool, I.R., Salem, E.T., Hassan, M.A., *International Journal of Modern Physics B*, **25**(8), 1081 (2011).
- [5] Ch. Fan, B. Poumellec, M. Lancry, X. He, H. Zeng, et al., *Opt Lett* **37**, 2955 (2012).
- [6] Salem, E.T., Ismail, R.A., Fakhry, M.A., Yusof, Y., *International Journal of Nanoelectronics and Materials* **9**(2), 111 (2016).
- [7] Z.T. Salim, U. Hashim, M.K.Md. Arshad, M.A. Fakhri, E.T. Salim, *Microelectron Eng*, **179**(5), 83 (2017).
- [8] X. Xu, Y. Q. Cao, P. Lu, J. Xu, W. Li, K. J. Chen, *IEEE Photon. J.* **6**(1), 2200207 (2014).
- [9] Meinan L., Dongfeng X., Shouchen Z., Haiyang Z., Jiyang W., Kenji K., *Mater. Lett.* **59**(8-9) 1095 (2005).
- [10] N. S. L. S. Vasconcelos, J. S. Vasconcelos, V. Bouquet, S. M. Zanetti, E. R. Leite, E. Longo, L. E. B. Soledade, F. M. Pontes, M. Guilloux-Viry, A. Perrin, M. I. Bernardi, J. A. Varela, *Thin Solid Films* **436**, 213 (2003).
- [11] Salem, E.T., Agool, I.R., Hassan, M.A., *International Journal of Modern Physics B* **25**(29), 3863 (2011).
- [12] Abdulrazaq, O.A., Saleem, E.T., *Turkish Journal of Physics* **30**(1), 35 (2006).
- [13] Makram A. Fakhri, Evan T. Salim, U. Hashim, Ahmed W. Abdulwahhab, Zaid T. Salim, *Journal of Materials Science: Materials in Electronics* **28**(22), 16728 (2017).
- [14] E.L. Wooten, K.M. Kissa, A. Yi-Yan, E.J. Murphy, D.A. Lafaw, P.F. Hallemeier, D. Maack, D.V. Attanasio, D.J. Fritz, G. J. McBrien, D.E. Bossi, *IEEE Journal of Selected Topics in Quantum Electronics* **6**, 69 (2000).
- [15] T. Zhang, B. Wang, Y. Zhao, S. Fang, D. Ma, Y. Xu, *Materials Chemistry and Physics* **88**, 97 (2004).
- [16] P. Galinetto, M. Marinone, D. Grando, G. Samoggia, F. Caccavale, A. Morbiato, M. Musolino, *Optics and Lasers in Engineering* **45**, 380 (2007).
- [17] W. Kim, S. Kwon, W. Jeong, G. Son, K. Lee, W. Choi, W. Yang, H. Lee, H. Lee, *Optics Express* **17**, 2638 (2009).
- [18] J. Guo, J. Zhu, W. Zhou, X. Huang, *Optics Communications*, **294**, 405 (2013).
- [19] A. Kadhim, Evan T. Salim, Saeed M. Fayadh, Ahmed A. Al-Amiery, Abdul Amir H. Kadhum, and Abu B. Mohamad, *The Scientific World Journal* **2014**, Article ID 490951 (2014).
- [20] D. Jannerl, D. Tulli, M. Garcia-Granda, M. Belmonte, V. Pruneri, *Laser & Photon. Rev.* **3**, 301 (2009).
- [21] M.R.R. Gesualdi, C. Jacinto, T. Catunda, M. Muramatsu, V. Pilla, *Appl. Phys. B* **93**, 879 (2008).
- [22] V. Ievlev, V. Shur, M. Sumets and A. Kostyuchenko, *Acta Metallurgica Sinica (English Letters)* **26**, 630 (2013).
- [23] P. Kumar, S M. Babui, S Perero, R. L. Sai, I Bhaumik, S Ganesamoorthy, A. K. Karnal, *Pramana J. Phys.* **75**, 1035 (2010).
- [24] N. E. Stankovaa, S. H. Tonchevb, E. Gyorgyc, G. Socolc, I. Mihailescuc, *J. Optoelectron. Adv. M.* **6**, 1345 (2014).
- [25] L. Chen, Q. Xu, M.G. Wood, R.M. Reano, *Optica* **1**, 112 (2014).

- [26] W. Kim, S.-W. Kwon, W. Jeong, G. Son, K. Lee, W. Choi, W. Yang, H. Lee, H. Lee, *Opt. Express* **17**, 2638 (2009).
- [27] Z.T. Salim, U. Hashim, M.K. Md Arshad, M.A. Fakhri, *Simulation, Int. J. Appl. Eng. Res.* **11**, 8785 (2016).
- [28] Z. Zhou, B. Wang, Sh. Lin, Y. Li and K. Wang, *Opt. Laser Technol.* **44**, 337 (2012).
- [29] P. Gangul, *Opt. Commun.* **285**(21/22), 4347 (2012).
- [30] Chen, H., T. Lv, A. Zheng, Y. Han, *Optics Communications*, **294**, 202 (2013).
- [31] W-K. Kim, S-W. Kwon, W-J. Jeong, G-S. Son, K-H. Lee, W-Y. Choi, W-S. Yang, H-M. Lee and H-Y. Lee, *Optics Express* **17**, 2638 (2009).
- [32] Y. Tan, F. Chen, M. Stepić, V. Shandarov, D Kip, *Optics Express* **16**, 10465 (2008).
- [33] H. K Lam, J. Y Dai, H. L. W Chan, *Journal of Crystal Growth* **268**, 144 (2004).
- [34] R. Grange, J-W. Choi, Ch-L. Hsieh, Y. Pu, A. Magrez, R. Smajda, L. Forró and D. Psaltis. *Applied Physics Letters* **95**, 143105 (2009).
- [35] Fakhri, M.A., Al-Douri, Y., Hashim, U., Salim, E.T., *Solar Energy* **120**, 381 (2015).
- [36] Y. Akiyama, K. Shitanaka, H. Murakami, Y. Shin, M. Yoshida, N. Imaishi, *Thin Solid Films* **515**, 4975 (2007).
- [37] Abood, M.K., Salim, E.T., Saimon, J.A., *International Journal of Nanoelectronics and Materials* **11**(2), 127 (2018).
- [38] R. Ageba, Y. Kadota, T. Maeda, N. Takiguchi, T. Morita, M. Ishikawa, *Journal of the Korean Physical Society* **57**, 918 (2010).
- [39] K. Peithmann, M. R. Zamani-Meymian, M. Haaks, K. Maier, B. Andreas, K. Buse, H. Modrow, *Appl. Phys. B.* **82**, 419 (2006).
- [40] E. R. Camargo, M. Kakihana, *Solid State Ionics* **151**, 413 (2002).
- [41] N. Ozer, C. M. Lampert, *Solar Energy Materials and Solar Cells* **39**, 367 (1995).
- [42] B. Knabe, D. Schu. Tze, T. Jungk, M. Svete, W. Ssenmacher, W. Mader, K. Buse, *Phys. Status Solidi A.* **208**, 857 (2011).
- [43] Makram A. Fakhri, Evan T. Salim, M. H. A. Wahid, U. Hashim, Zaid T. Salim, *Journal of Materials Science: Materials in Electronics* **29**(11), 9200 (2018).
- [44] Halboos, H.T., Salim, E.T, *IOP Conference Series: Materials Science and Engineering* **454**(1) (2018).
- [45] Makram A.Fakhri, Evan T.Salim, Ahmed W.Abdulwahhab, U.Hashim, Zaid T.Salim, *Optics and Laser Technology* **103**, 226 (2018).
- [46] Makram A Fakhri, Y Al-Douri, Evan T Salim, Uda Hashim, Yushamdan Yusof, EeBee Choo, Zaid T Salim, Yaseen N Jurn, *ARPN J. Eng. Appl. Sci* **11**, 4974 (2016).
- [47] Evan T Salim, Jehan Admon Saimon, Marwa K Abood, Makram A Fakhri, *Materials Research Express* **4**(10), 106407 (2017).
- [48] V. Ievlev, M. Sumets, A. Kostyuchenko, N. Bezryadin, *Journal of Materials Science: Materials in Electronics* **24**, 1651 (2013).
- [49] Y. Kang, S. Jeong, S. Lee, J. Hwang, J. Kim, C. Cho, *Journal of the Korean Physical Society*, **49**, S625 (2006).
- [50] Evan T. Salim, Marwa S. Al-Wazny, Makram A. Fakhri, *Modern Physics Letters B*, **27**(16), 1350122 (2013).
- [51] Salim, E.T., *International Journal of Nanoelectronics and Materials* **5**(2), 95 (2012).
- [52] Salim, E.T., *Indian Journal of Physics* **87**(4), 349 (2013).